Nuclear Mathematical and Computational Sciences: A Century in Review, A Century Anew
Gatlinburg, Tennessee, April 6-11, 2003, on CD-ROM, American Nuclear Society, LaGrange Park, IL (2003)

ANALYSIS OF THE NRC PCA PRESSURE VESSEL DOSIMETRY BENCHMARK USING TRIPOLI-4.3 MONTE CARLO CODE AND ENDF/B-VI.4, JEF2.2 AND IRDF-90 LIBRARIES

Y. K. Lee
CEA/Saclay –DEN/DM2S/SERMA/LEPP
91191 Gif sur Yvette Cedex, France
yklee@cea.fr

ABSTRACT

The fast neutron induced embrittlement of the reactor pressure vessel (RPV) is the main cause limiting the PWR lifetime. The ORNL Pool Critical Assembly (PCA) pressure vessel simulator benchmark has been formulated in NUREG report and entitled as US NRC Benchmark in SINBAD database. This paper reports on calculations made on this PCA benchmark using 3-D TRIPOLI-4.3 Monte Carlo transport code. Continuous energy cross-section libraries ENDF/B-VI.4 and JEF2.2 were separately investigated in transport calculations. Different reactor dosimetry files, IRDF-90, IRDF-90.v2, RRDF-98 and JENDL/D-99 were also tested in detector reaction rate calculations. Reaction rates for the ^{27}Al(n,α), ^{58}Ni(n,p), ^{238}U(n,f), ^{237}Np(n,f), ^{115}In(n,n'), and ^{103}Rh(n,n') reactions, and integral neutron fluxes for the energies above 1 and 0.1 MeV were analyzed in seven key reactor capsule locations of the RPV simulator. The results of this study show a good agreement between calculations and experiments for most capsule locations. At large depths in the RPV, the under prediction about 10% was observed for ^{27}Al(n,α) and ^{103}Rh(n,n') detectors when using ENDF/B-VI.4 data file. The Fe inelastic scattering cross section and the tail of the ^{235}U fission spectrum are two important factors to take into account for ^{27}Al(n,α) detector.

Key Words: PCA Benchmark, Neutron transport, TRIPOLI-4, PWR Pressure Vessel, Monte Carlo

1. INTRODUCTION

The fast neutron induced embrittlement of the reactor pressure vessel (RPV) is the main cause limiting the PWR lifetime. Improving the calculation methodology and reducing the uncertainty in the RPV fluence estimate have a direct impact on the operation limits of the reactors [1]. At CEA /Saclay, RPV dosimetry was analyzed using the 3-D Monte Carlo code TRIPOLI-3 with multi-group ENDF/B-VI library and International Reactor Dosimetry File IRDF-85 [2]. Recently, the continuous energy TRIPOLI-4 code and IRDF-90 file have been introduced for RPV dose calculations. New features like lattices geometry, point-wise cross-section, automatic variance reduction and parallel implementation in TRIPOLI-4 and recent advances in computer capabilities make the Monte Carlo RPV dosimetry calculations to be more accurate and practical.

RPV dosimetry related benchmarks, ASPIS (1 m thick Iron), PCA-REPLICA (Water/Iron, 12/13 configuration), NESDIP-3 (Water/Iron, 18/20 configuration), Winfrith Water (50 cm thick Water) and Saint-Laurent B1 PWR RPV surveillance results [1-3], were routinely calculated before each release of TRIPOLI codes. These benchmarks validate not only the cross-sections and their processing but also the transport calculations and their variance reduction schemes. To develop

the database of RPV dosimetry benchmarks for the TRIPOLI code, more NRC certified benchmarks are currently being investigated [4].

The ORNL Pool Critical Assembly (PCA) RPV simulator benchmark has been formulated in NUREG report and entitled as US NRC Benchmark in SINBAD database [5]. Its purpose was to validate the capabilities of the calculation methodology to predict the reaction rates in the region outside a reactor core when the neutron source, material compositions, and geometry are well defined. Comparing with UKAEA PCA-REPLICA benchmark (using only ^{103}Rh(n,n'), ^{115}In(n,n') and ^{32}S(n,p) detectors), more useful dosimeters of different threshold energies were used in ORNL PCA benchmark. Besides, the PCA neutron source only comes from the reactor core and the background noise correction, about 4% in PCA-REPLICA, is not necessary.

In the past years, the PCA benchmark was widely used for qualifying 3-D Sn synthesis method, real 3-D Sn transport calculations and related multi-group cross-section libraries [4-9]. According to the study in Ref. 7, the real 3-D analysis is necessary to account for transverse leakage effects in this small reactor while the 3-D Sn synthesis approach, which combines 2-D and 1-D Sn calculations, under-predicts reaction rates at large depths in the RPV simulator.

Different 3-D Monte Carlo transport calculations were also reported for this PCA benchmark using MCBEND and MCNP codes [8, 9]. Early MCBEND results presented the uncertainties about 5% and introduced the correction factors up to 7% due to its 2 cm thick volume estimators. Early MCNP-3A results showed an underestimation of 10% to 35% using ENDF/B-V library and a limit of its biasing techniques for ^{27}Al(n,α) detector.

This paper reports on calculations made on this PCA benchmark using continuous-energy TRIPOLI-4.3 code [10]. Cross-section libraries ENDF/B-VI.4 and JEF2.2 were separately investigated in transport calculations. Detector cross-sections from different reactor dosimetry files, IRDF-90, IRDF-90.v2, RRDF-98 and JENDL/D-99 [16], and from cross-section libraries ENDF/B-VI.4 and JEF2.2, were also utilized and compared in this study to improve the calculation results. Reaction rates for the ^{27}Al(n,α), ^{58}Ni(n,p), ^{238}U(n,f), ^{237}Np(n,f), ^{115}In(n,n') and ^{103}Rh(n,n') reactions, and integral neutron fluxes for the energies above 1 and 0.1 MeV were analyzed in seven key reactor capsule locations of the RPV simulator.

2. DESCRIPTION OF THE PCA PRESSURE VESSEL BENCHMARK

The PCA pressure vessel benchmark mocked up the core-to-cavity region in a PWR. The PCA 12/13 configuration is geometrically similar to the downcomer I - thermal shield - downcomer II – pressure vessel – reactor cavity design [5, 6, 8].

A horizontal cross section of the PCA benchmark, showing characteristics of the core axial mid-plane materials, is presented in Figure 1. The main components included a PCA core, a thermal shield, a pressure vessel simulator, and a void box to simulate the reactor cavity. The facility was located in a large pool of water, which serves as reactor core moderator and provides shielding. A section view through the center of the mockup is shown in Figure 2. The 8 vertical experimental access tubes in which the measurements were done were filled with appropriate material (steel in

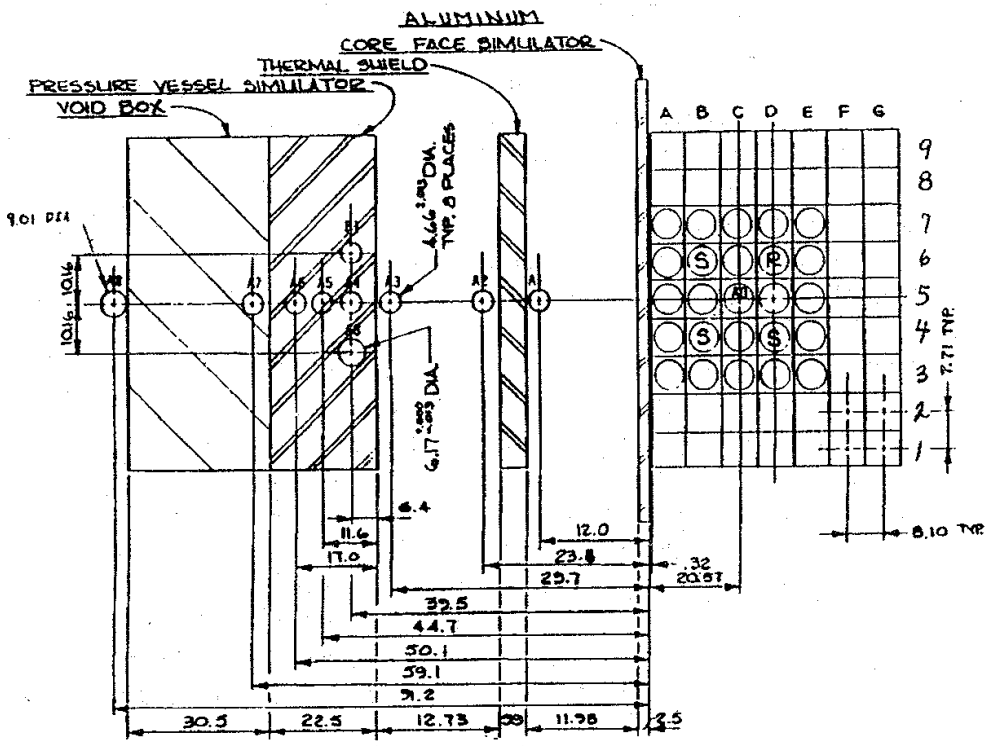

Figure 1. PCA 12/13 configuration – X-Y geometry

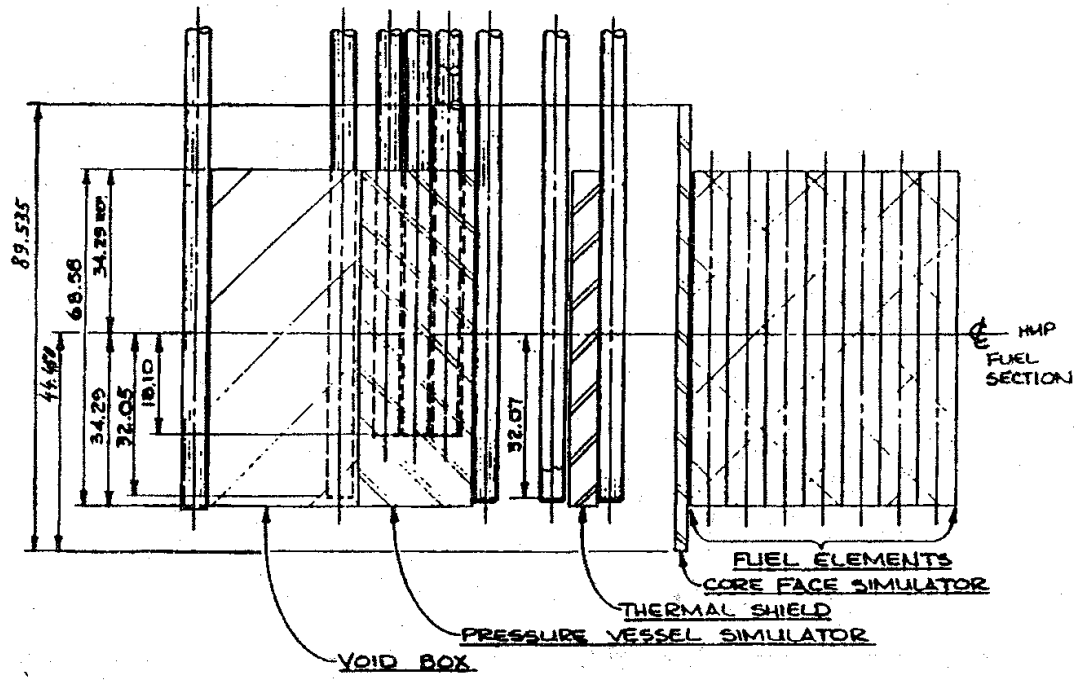

Figure 2. PCA 12/13 configuration – Y-Z geometry

the pressure vessel locations and Plexiglas in the in-water locations) in order to minimize the perturbations of the neutron field. References 5 and 6 provide the detailed data for this benchmark.

2.1. PCA neutron source

The PCA reactor core was composed of 25 (5x5) material testing reactor (MTR) plate-type fuel elements. Fresh fuel with 93% ^{235}U enrichment was used so as to reduce the burn-up and the fission product effects on neutron source distribution. Three types of fuel elements (70, 140 or 220 g ^{235}U) were presented in the core but on the first row facing the experiment only standard fuel elements (140 g ^{235}U) were loaded.

The pitch between two fuel elements is 7.71 cm in X direction and 8.10 cm in Y direction and it was given in Fig. 1. The height of the fissile materials is only 60.008 cm. The power distribution of the fuel elements was obtained from fission chamber measurements and core calculations. As a part of the benchmark specification, in the horizontal plane, it was provided as an array of relative power densities (3 x 3 values per fuel element). In the vertical direction, the cosine-shaped distribution was also specified in Ref. 5.

2.2. RPV Simulator and 12/13 configuration

The thickness of the water gap (downcomer I) on the core side of the thermal shield is 11.98 cm. The 12.73 cm water gap (downcomer II) was designed to separate the thermal shield and the RPV simulator. For this reason the configuration used for this benchmark was labeled as 12/13 configuration. The thickness of the stainless steel thermal shield and the carbon steel pressure vessel is 5.9 cm and 22.5 cm, respectively. The dimensions of the thermal shield slab and the RPV slab are 68.58 cm x 68.58 cm. The simulated reactor cavity (void box), with dimensions 68.58 cm x 30.48 cm x 68.58 cm, was positioned behind the pressure vessel mockup. A core aluminum window of 2.5 cm thickness was introduced to simulate core face.

2.3. Reaction rates measurement

During the PCA experiments, measurements were taken at several locations within the mockup to provide traverse data extending from the reactor core outward through the pressure vessel simulator and on into the void box. Measured data were supplied for a variety of reactions with responses spanning the fast neutron energy range.

Measurements were performed at the core mid-plane and labeled in Fig. 1 as A1 to A7. Data from locations A1 to A3 allow to study the attenuation of fast neutron dose by thermal shield and by water gap of downcomer II and data from A3 to A7 to examine the calculated gradient of fast neutron dose within the pressure vessel wall.

^{103}Rh(n,n'), ^{115}In(n,n'), ^{58}Ni(n,p) and ^{27}Al(n,α) reaction rates were determined with activation monitors while fission chambers and solid state track recorders (SSTR) were used to evaluate the ^{237}Np(n,f) and ^{238}U(n,f) fission rates. The photo-fission corrections were also considered for ^{237}Np and ^{238}U fission rate measurements.

3. TRIPOLI-4.3 CALCULATION MODEL

The Monte Carlo radiation transport code TRIPOLI-4 was described in Ref. 10. Its point-wise representation of nuclear data applied on reactor physics analysis and on ^{235}U and ^{238}U cross-section benchmarks, was demonstrated in Ref. 11. Its powerful lattice features applied on simple pin-by-pin model for storage arrays and on complex plate-by-plate model for MTR reactor core were established in Refs 12 and 13. Its automatic biasing techniques and parallel computing capabilities were described in Refs 14 and 15. In order to obtain the finest results with TRIPOLI-4.3 calculation, the above cited techniques were largely applied on this PCA benchmark.

3.1. Geometry model, material compositions and neutron source

According to the Figures 1.4 and 1.6 of Ref. 5, the PCA core was exactly described with the TRIPOLI-4.3 so as to take into account the fuel plate curvature, the water layers between fuel plates, the cooling channel interface between the PCA fuels and the core aluminum window. Both standard fuel elements with 18 bended fuel plates and control-rod fuel elements with 9 fuel plates were plate-by-plate modeled. A 5x5 mixture of standard fuel lattice and control-rod fuel lattice was made to describe the PCA core. The RPV simulator geometry including thermal shield and 12/13 configuration was also exactly described using combinatorial geometry without taking advantage of the problem symmetry.

The material compositions and the horizontal relative power density distribution (3 x 3 values per fuel element) were taken from Tables 1.2 - 1.5 of Ref. 5. The cosine-shaped vertical power density distribution was taken from formula 1.1 of Ref. 5. The PCA core average buckling B_z is 4.42 E-2 cm^{-1} and the maximum of the vertical distribution lies 4.2 cm below the core horizontal mid-plane due to the partial insertion of the control rods from the top of the core. TRIPOLI-4.3 shielding calculations, using above cited 3-D neutron source distribution, were normalized to one neutron/second from the PCA core. A ^{235}U Watt fission spectrum was utilized in this study with thermal neutron spectrum parameters a=0.988 and b=2.249.

3.2. Cross-section libraries and reaction rates calculations

Two continuous energy cross-section libraries from ENDF/B-VI.4 and JEF2.2 were separately used in TRIPOLI-4.3 transport calculations. They were prepared by NJOY/94.105 processing system using RECONR and BROADR modules with the convergence criteria 0.1% [10, 11].

The tally disks were 5 cm in radius and 0.0005 cm thick in the plane perpendicular to the flow of neutron. Point estimators were also used to verify the coherence of the results with the surface estimators. The distances D from the core surface of the aluminum window to the tally surface are taken from the Table 1.6 of Ref. 5 and given in the Fig. 1 and Table I.

Both the neutron fluxes above 1 and 0.1 MeV and the reaction rate calculations were obtained in the same run. The detector cross-sections from different reactor dosimetry files, IRDF-90, IRDF-90.v2, RRDF-98 and JENDL/D-99 were studied to improve the calculation results. ENDF/B-VI.4 and JEF2.2 data files were also tested to obtain detector responses. These tests can identify how they differ from the above cited reactor dosimetry files in RPV dose calculations.

3.3. Variance reduction techniques

The TRIPOLI codes use several variance reduction schemes like exponential transform, splitting, Russian roulette and quota sampling [14]. An automatic importance graph generator called INIPOND is available in TRIPOLI to simplify the variance reduction work [10].

In this study, an importance function defined on a 3-D mesh was generated with 30000 neutron histories. The INIPOND module produced the importance graph according to the mesh structure, the material compositions, the neutron energy grid and the detector locations. The collapsed cross sections are transport corrected to account for deviations from diffusive flow.

The mesh size used in INIPOND was 6.8 cm x 4.4 cm x 5.9 cm. The smaller the mesh size the longer CPU time and the bigger memory are needed to generate a 3-D importance function. The 4.4 cm mesh thickness that is smaller than the thermal shield thickness (5.9 cm), allows to efficiently and correctly calculate the fast neutron attenuation in this 12/13 configuration.

The threshold energies for the ^{27}Al(n,α), ^{58}Ni(n,p), ^{238}U(n,f), ^{237}Np(n,f), ^{115}In(n,n') and ^{103}Rh(n,n') reactions are 5.0, 2.1, 1.5, 0.7, 0.3 and 0.1 MeV respectively. A four-group energy grid (20. - 4. - 2. - 1. - 0.1 MeV) was used for generating the importance map. This energy grid was a compromise to obtain converged results (standard deviation less than 1%) in the same run

Table I. Measured reaction rates – PCA 12/13 configuration

Midplane Location[§]	D (cm)	Reaction Rate per PCA core Neutron [+&] ^{103}Rh(n,n')	^{115}In(n,n')	^{58}Ni(n,p)	^{27}Al(n,α)	^{237}Np(n,f)	^{238}U(n,f)
TSF (A1)	12.0	4.06 E-30	1.05 E-30	6.31 E-31	5.48 E-33	-----	-----
TSB (A2)	23.8	4.50 E-31	1.14 E-31	6.72 E-32	7.16 E-34	-----	-----
PVF (A3)	29.7	1.47 E-31	3.68 E-32	2.50 E-32	3.13 E-34	2.98 E-31*	6.05 E-32*
1/4 T (A4)	39.5	5.67 E-32*	1.11 E-32	5.69 E-33	7.15 E-35	1.20 E-31	1.79 E-32
1/2 T (A5)	44.7	3.24 E-32	5.20 E-33	2.25 E-33	2.92 E-35	6.56 E-32	7.88 E-33
3/4 T (A6)	50.1	1.67 E-32	2.23 E-33	7.99 E-34	1.12 E-35	3.47 E-32	3.26 E-33
VB (A7)	59.1	4.83 E-33	6.43 E-34	-----	4.29 E-36	9.60 E-33	8.65 E-34

+ Recommended values from Table 6.2.1 and Table 6.1.2 of Ref. 8.
& Overall combined uncertainties for ^{103}Rh, ^{115}In, ^{58}Ni and ^{27}Al reaction rates are about ±6%. For the ^{237}Np and ^{238}U, the combined uncertainties from fission chamber and solid state track recorder measurements are about ±10%.
* Values taken from Table 1.6 of Ref. 5 or Table 5.3.1 of Ref. 8.
§ TSF : Thermal Shield Front, TSB : Thermal Shield Back, PVF : Pressure Vessel Front,
¼ T : ¼ Thickness of RPV, 1/2 T : 1/2 Thickness of RPV, 3/4 T : 3/4 Thickness of RPV, VB : Void Box.

for five different detector responses. A cutoff energy of 0.1 MeV was used in order to reduce the cost of the calculation. For $^{27}Al(n,\alpha)$ reaction, an higher cutoff energy of 5 MeV and a two-group energy grid (20. - 8. - 5. MeV) were set in a separated run so as to obtain converged results. For each run 50 million neutron histories were simulated.

4. RESULTS AND COMPARISONS

As the measured results were not totally presented in Table 1.6 of Ref 5, recommended values of measured reaction rates from Tables 6.1.2 and 6.2.1 of Ref. 8 are directly utilized in Table I. A few exceptions are taken from Table 5.3.1 of Ref. 8 (location A4 – reaction rate $^{103}Rh(n,n')$ and location A3 – fission rate $^{238}U(n,f)$) and from Table 1.6 of Ref. 5 (location A3 – fission rate $^{237}Np(n,f)$). TRIPOLI-4.3 calculated reaction rates are reported in Tables II.1 and II.2. Calculated to experimental (C/E) ratios are also presented using the measured reaction rates of Table I.

Table II.1 Reaction rate comparisons: TRIPOLI-4.3 and Experimental

Reaction Rate per PCA core Neutron *

Location	Library	$^{103}Rh(n,n')$	C/E	$^{115}In(n,n')$	C/E	$^{58}Ni(n,p)$	C/E
A1	ENDF/B-VI	3.90 E-30 ± 0.2%	0.96	9.61 E-31± 0.2%	0.92	5.78 E-31± 0.2%	0.92
	JEF2.2	4.01 E-30 ± 0.2%	0.99	9.89 E-31± 0.3%	0.94	5.95 E-31± 0.4%	0.94
A2	ENDF/B-VI	4.54 E-31 ± 0.4%	1.01	1.07 E-31± 0.3%	0.94	6.41 E-32± 0.5%	0.95
	JEF2.2	4.63 E-31 ± 0.3%	1.03	1.10 E-31± 0.3%	0.96	6.52 E-32± 0.5%	0.97
A3	ENDF/B-VI	1.49 E-31 ± 0.5%	1.01	3.68 E-32± 0.4%	1.00	2.44 E-32± 0.6%	0.98
	JEF2.2	1.53 E-31 ± 0.5%	1.04	3.80 E-32± 0.6%	1.03	2.50 E-32± 0.8%	1.00
A4	ENDF/B-VI	5.57 E-32 ± 0.6%	0.98	1.10 E-32± 0.6%	0.99	5.46 E-33± 0.9%	0.96
	JEF2.2	5.62 E-32 ± 0.6%	0.99	1.11 E-32± 0.9%	1.00	5.39 E-33± 0.9%	0.95
A5	ENDF/B-VI	2.99 E-32 ± 0.5%	0.92	5.04 E-33± 0.6%	0.97	2.13 E-33± 1.0%	0.95
	JEF2.2	2.95 E-32 ± 0.4%	0.91	5.06 E-33± 0.6%	0.97	2.11 E-33± 0.9%	0.94
A6	ENDF/B-VI	1.49 E-32 ± 0.5%	0.89	2.17 E-33± 0.7%	0.97	8.04 E-34± 1.2%	1.01
	JEF2.2	1.47 E-32 ± 0.5%	0.88	2.19 E-33± 0.8%	0.98	7.79 E-34± 1.2%	0.97
A7	ENDF/B-VI	4.45 E-33 ± 0.4%	0.92	6.01 E-34± 0.7%	0.93	2.13 E-34± 1.4%	----
	JEF2.2	4.21 E-33 ± 0.4%	0.87	5.85 E-34± 0.7%	0.91	2.04 E-34± 1.4%	----

* $^{103}Rh(n,n')$: RRDF-98, $^{115}In(n,n')$ and $^{58}Ni(n,p)$: IRDF-90.

The disparity and the trend of the C/E ratios from location A1 to A7 are helpful to identify the impact of nuclear data libraries. Both ENDF/B-VI.4 and JEF2.2 results are presented in the near place so that their differences are easy to evaluate. The most favorable dosimetry files are also utilized for each of the six detectors to report the TRIPOLI-4.3 calculation results.

In Table II.1 the calculated reaction rates of the ^{103}Rh(n,n'), ^{115}In(n,n') and ^{58}Ni(n,p) reactions are given and the C/E ratios of ENDF/B-VI.4 are generally comparable with those of JEF2.2 at locations A4, A5 and A6. Due to the Fe cross sections, the C/E ratios of JEF2.2 are about 6% lower at location A7 for ^{103}Rh(n,n') and ^{58}Ni(n,p) detectors.

For ^{103}Rh(n,n') detector, the RRDF-98 data can improve C/E ratios of 2 to 4% from location A1 to A5 comparing with IRDF-90. But the C/E ratio degrades about 10% through the thick pressure vessel for both RRDF-98 and IRDF-90. The ^{103}Rh(n,n') cross sections from RRDF-98 will be also suggested for IRDF-2002 [16]. The ^{103}Rh(n,n') cross sections in ENDF/B-VI.4 and JEF2.2 are not accurate enough for the present study because they produce unacceptable C/E ratios.

Table II.2 Reaction rate comparisons: TRIPOLI-4.3 and Experimental

Reaction Rate per PCA core Neutron *

Location	Library	^{27}Al(n,α)	C/E+	^{237}Np(n,f)	C/E	^{238}U(n,f)	C/E
A1	ENDF/B-VI	5.11 E-33 ± 0.4%	0.93	7.25 E-30± 0.2%	----	1.59 E-30± 0.3%	----
	JEF2.2	5.14 E-33 ± 0.3%	0.94	7.43 E-30± 0.2%	----	1.63 E-31± 0.3%	----
A2	ENDF/B-VI	6.84 E-34 ± 0.5%	0.96	8.60 E-31± 0.3%	----	1.76 E-31± 0.5%	----
	JEF2.2	6.70 E-34 ± 0.5%	0.94	8.74 E-31± 0.3%	----	1.81 E-31± 0.3%	----
A3	ENDF/B-VI	3.04 E-34 ± 0.5%	0.97	2.74 E-31± 0.4%	0.92	6.18 E-32± 0.6%	1.02
	JEF2.2	2.97 E-34 ± 0.6%	0.95	2.81 E-31± 0.5%	0.94	6.40 E-32± 0.6%	1.06
A4	ENDF/B-VI	6.67 E-35 ± 0.7%	0.93	1.15 E-31± 0.5%	0.96	1.71 E-32± 0.7%	0.96
	JEF2.2	6.20 E-35 ± 0.6%	0.87	1.15 E-31± 0.5%	0.96	1.74 E-32± 1.0%	0.97
A5	ENDF/B-VI	2.66 E-35 ± 0.8%	0.91	6.44 E-32± 0.5%	0.98	7.37 E-33± 0.7%	0.94
	JEF2.2	2.42 E-35 ± 0.7%	0.83	6.31 E-32± 0.4%	0.96	7.50 E-33± 0.6%	0.95
A6	ENDF/B-VI	9.93 E-36 ± 0.9%	0.89	3.32 E-32± 0.4%	0.96	3.03 E-33± 0.8%	0.93
	JEF2.2	9.09 E-36 ± 0.9%	0.81	3.23 E-32± 0.4%	0.93	3.08 E-34± 0.9%	0.94
A7	ENDF/B-VI	3.28 E-36 ± 1.2%	0.77	1.01 E-32± 0.4%	1.05	7.98 E-34± 0.8%	0.92
	JEF2.2	2.88 E-36 ± 1.2%	0.67	9.39 E-33± 0.4%	0.98	8.00 E-34± 0.9%	0.92

* ^{27}Al(n,α): IRDF-90.v2, ^{237}Np(n,f): JENDL/D-99, ^{238}U(n,f): IRDF-90.

For ^{103}Rh detector, different experimental results at locations A4 and A6 were also found. The differences are 12% at A4 and 4% at A6 between Table 1.6 of Ref. 5 and Table 6.2.1 of Ref. 8.

For ^{115}In and ^{58}Ni detectors, the C/E ratios using IRDF-90 were reported and they are excellent from location A4 to A6. The cross sections of ^{115}In(n,n') from ENDF/B-VI.4 and IRDF-85 under predict about 5% with comparison with those from IRDF-90 and those from JEF2.2 are of little use. The ^{58}Ni(n,p) cross sections from ENDF/B-VI.4 and IRDF-90 produce the same results.

In Table II.2 the calculated reaction rates of ^{27}Al(n,α), ^{237}Np(n,f) and ^{238}U(n,f) are reported. Like in Table II.1, the C/E ratios of JEF2.2 library are higher within 2-4% from location A1 to A3 and the C/E ratios using JEF2.2 library are similar to those using ENDF/B-VI.4 from location A4 to A6 except for the ^{27}Al(n,α) detector.

For energy above 5 MeV, the Fe inelastic scattering cross sections from JEF2.2 are not accurate enough so the C/E ratios of the ^{27}Al(n,α) detector are only about 0.8 at location A5 and A6. The improvement of C/E ratios by using ENDF/B-VI.4 in transport calculation is clear for ^{27}Al(n,α) reaction rates but unsatisfactory because the C/E ratio still degrades about 20% through the thick RPV (from location A3 to A7).

The ^{27}Al(n,α) cross sections from IRDF-90.v2 and ENDF/B-VI.4 produce the same results and they are still suggested for IRDF-2002 [16]. The obvious underestimation at locations A5, A6 and A7 for the ^{27}Al(n,α) detector was also observed in early MCBEND and THREEDANT calculations [8, 9] but this evident degradation of C/E ratios was not reported in recent TORT calculation [7] and in recent DORT synthesis approach [5]. These above observations propose that for ^{27}Al(n,α) reaction rate calculations, the ^{235}U fission spectrum from ENDF/B-VI library [17] could be also helpful to improve the under prediction at location A5, A6 and A7.

For ^{237}Np(n,f) detector, the JENDL/D-99 data allow to improve C/E ratios from 3.3% at location A4 up to 5.7% at A7 comparing with continuous energy data from ENDF/B-VI.4. These C/E ratio improvements are also about 3-5% from location A4 to A7 if using IRDF-90 instead of ENDF/B-VI.4. The ^{237}Np(n,f) cross sections from the JENDL/D-99 file were also suggested in Ref. 16 because the uncertainty in JENDL/D-99 is much smaller comparing with IRDF-90.

For locations within the RPV wall the C/E ratios of ^{238}U(n,f) detector were improved about 5% when using averaged measurement results based on the SSTR recorders and the fission chambers instead of only using the fission chambers results [5-8]. But the under prediction of 4-8% for ^{238}U(n,f) detector by calculation is still clear in the RPV wall and the degradation of C/E ratios from location A3 to A7 is about 10% for ENDF/B-VI.4 and about 14% for JEF2.2.

4.1. Calculated and measured integral neutron fluxes

Calculated and measured integral neutron fluxes above 1 and 0.1 MeV are reported in Table III. The experimental ones are taken from Table 7.1.3.1 of Ref. 8 and they were derived from consistency analysis of PCA detector measurements (SSTR, activation monitor and fission chamber). For locations A1 and A3, the measured integral neutron fluxes were not reported in Table 7.1.3.1 of Ref. 8 so they are taken directly from Table 2 of Ref. 9.

Table III. Integral neutron flux comparisons: TRIPOLI-4.3 and Experimental

	Neutron flux per PCA core Neutron									
	(a) Neutron energy above 1.0 MeV					(b) Neutron energy above 0.1 MeV				
Location	TRIPOLI	Std.	Exp.[+]	Std.	C/E	TRIPOLI	Std.	Exp.[+]	Std.	C/E
TSF (A1)										
ENDF/B-VI.4	3.57 E-6	± 0.3%	3.71 E-6	± ---	0.96	6.42 E-6	± 0.3%	6.94 E-6	± ---	0.93
JEF2.2	3.67 E-6	± 0.3%			0.99	6.59 E-6	± 0.2%			0.95
TSB (A2)										
ENDF/B-VI.4	4.06 E-7	± 0.4%	4.01 E-7	± 10%	1.01	8.12 E-7	± 0.3%	---- E-7	± ---	---
JEF2.2	4.15 E-7	± 0.3%			1.03	8.19 E-7	± 0.2%			---
PVF (A3)										
ENDF/B-VI.4	1.35 E-7	± 0.5%	1.33 E-7	± ---	1.02	2.42 E-7	± 0.4%	2.49 E-7	± ---	0.97
JEF2.2	1.40 E-7	± 0.6%			1.05	2.46 E-7	± 0.4%			0.99
¼ T (A4)										
ENDF/B-VI.4	4.48 E-8	± 0.6%	4.50 E-8	± 6%	1.00	1.28 E-7	± 0.4%	1.35 E-7	± 11%	0.95
JEF2.2	4.49 E-8	± 0.8%			1.00	1.33 E-7	± 0.4%			0.99
½ T (A5)										
ENDF/B-VI.4	2.15 E-8	± 0.7%	2.21 E-8	± 6%	0.97	8.30 E-8	± 0.4%	9.01 E-8	± 12%	0.92
JEF2.2	2.12 E-8	± 0.5%			0.96	8.57 E-8	± 0.3%			0.95
¾ T (A6)										
ENDF/B-VI.4	9.48 E-9	± 0.7%	9.73 E-9	± 8%	0.97	4.88 E-8	± 0.3%	5.37 E-8	± 15%	0.91
JEF2.2	9.30 E-9	± 0.7%			0.96	5.08 E-8	± 0.3%			0.95
VB (A7)										
ENDF/B-VI.4	2.64 E-9	± 0.5%	2.88 E-9	± 43%	0.92	1.55 E-8	± 0.3%	1.70 E-8	± 47%	0.91
JEF2.2	2.50 E-9	± 0.6%			0.87	1.55 E-8	± 0.3%			0.91

+ Experimental values taken from Table 7.1.3.1 of Ref. 8 and, for location A1 and A3, taken from Table 2 of Ref. 9.

In Table III, the TRIPOLI-4.3 C/E ratios for integral neutron flux above 1 MeV are excellent when using ENDF/B-VI.4 or JEF2.2 libraries. At location A7, where the uncertainty of experimental result is very important, the C/E ratios degrade. Due to the RPV simulator, the C/E ratios from location A3 to A7 degrade down 10% with ENDF/B-VI.4 and 18% with JEF2.2. These degradations are already observed in Tables II.1 and II.2 with ^{238}U(n,f), ^{115}In(n,n'), ^{103}Rh(n,n') and ^{27}Al(n,α) detectors. For the integral neutron flux above 0.1 MeV, the C/E ratios are also good using these two cross section libraries but their degradation within 6 - 8% from A3 to A7 indicates once again that the improvement for Fe cross sections around 1 MeV may be necessary.

From location A1 (thermal shield front) to A7 (void box), the attenuation of integral flux above 1 MeV results in a reduction factor of 1350. The integral flux gradient within the RPV wall is also interesting to evaluate and, from location A3 (pressure vessel front) to A7, the reduction factor is

about 50. The attenuation of integral flux above 0.1 MeV results in a reduction factor of only 400 from location A1 to A7. Due to the neutron scattering in the RPV simulator and the soft-down of neutron spectrum, the flux ratio (b)/(a) in Table III increases rapidly from 2 at A2 up to 6 at A7.

5. CONCLUSIONS

It is interesting to investigate the PCA benchmark with 3-D Monte Carlo code TRIPOLI-4.3 and different reactor dosimetry files because, firstly, the PCA core and related 3-D power distribution were exactly described in the NUREG benchmark report and, secondly, the ^{237}Np(n,f), ^{238}U(n,f), ^{58}Ni(n,p) and ^{27}Al(n,α) detectors were not utilized in the geometrically similar benchmarks PCA-REPLICA and NESDIP-3 while three of these dosimeters are used in the French PWR reactor vessel surveillance program.

This study using continuous energy libraries from ENDF/B-VI.4 and JEF2.2 to calculate RPV simulator dosimetry is also worth to note because it is important to free Monte Carlo transport calculations from multi-group energy structure. The self-shielding calculation, the weighting spectra consideration and the adjustment of cross-sections are not necessary. The automatic variance reduction and the parallel computing in TRIPOLI-4.3 code also facilitate this study.

The IRDF-90 file is generally good for RPV dosimetry calculation but to improve the C/E ratios, the cross sections of ^{103}Rh(n,n') and ^{237}Np(n,f) from RRDF-98 and JENDL/D-99 respectively are recommended. Comparing with measured ^{237}Np(n,f) and ^{238}U(n,f) fission rates reported in NUREG report [5], the experimental results utilized in References 7 and 8 are recommended as they can clearly improve C/E ratios at RPV wall.

The results of this study show a good agreement between calculations and experiments for most capsule locations. At large depths in the RPV, the under prediction about 10% was observed for ^{27}Al(n,α) and ^{103}Rh(n,n') detectors when using ENDF/B-VI.4 library. This study also confirms that, for neutron energy above 5 MeV, the Fe inelastic scattering cross sections from ENDF/B-VI.4 are more accurate than those from JEF2.2. More study on Fe inelastic scattering cross sections may be necessary to improve the fast neutron flux prediction at large depths in the RPV.

An additional interesting point concerning the tail above 10 MeV of the ^{235}U fission spectrum is currently investigated [17]. The first results show that, for this PCA benchmark, it is helpful to improve the C/E ratios for ^{27}Al(n,α) detector. This potential improvement of C/E ratios for high energy detector like ^{63}Cu(n,α) will be also attractive for PWR RPV dosimetry estimate [18].

ACKNOWLEDGMENTS

The author would like to thank Dr. I. Remec (ORNL), Dr. E. M. Zsolnay (Budapest University), Dr. C. M. Diop and Mr. M. Chiron (CEA) for fruitful discussions on RPV dosimetry calculation, and Mr. Q. L. Mei (SNERDI, China) for preparing the geometry of the PCA core.

REFERENCES

1. "Computing Radiation Dose to Reactor Pressure Vessel and Internals: State-of-the-Art Report ", NEA/NSC/DOC (96) 5, pp. 28-38, (1997).
2. J. C. Nimal et al., "French PWR 900 MWe Pressure Vessel Surveillance - Neutron Field Characteristics - TRIPOLI-3 Calculations and Experimental Determination", *The 8th Int. Conf. on Radiation Shielding (8th ICRS)*, Arlington, TX, 24-28 April, pp.699-705 (1994).
3. "SINBAD – an International Database for Integral Shielding Experiments", http://www.nea.fr/html/science/shielding/sinbad/sinbadi.htm (2003).
4. I. Remec, "Two Benchmarks for Qualification of Pressure Vessel Fluence Calculational Methodology", *Proc. ANS Radiation Protection & Shielding Topical Conference*, Nashville, TN, April, 1998, Vol. 1. pp.295-302. See also ORNL/CP-96966 (1998).
5. I. Remec and F. B. K. Kam, "Pool Critical Assembly Pressure Vessel Facility Benchmark", NUREG/CR-6454, (ORNL/TM-13205), USNRC, July (1997).
6. W. N. McElroy, Ed., "LWR Pressure Vessel Surveillance Dosimetry Improvement Program : PCA Experiments and Blind Test", NUREG/CR-1861, USNRC, July (1981).
7. A. H. Fero et al., "Analysis of the ORNL PCA Benchmark Using TORT and BUGLE-96", *The 10th Int. Symposium on Reactor Dosimetry (10th ISRD)*, Osaka, Japan, 12-17 Sept., pp.360-366 (1999).
8. W. N. McElroy, Ed., "LWR Pressure Vessel Surveillance Dosimetry Improvement Program : PCA Experiments, Blind Test and Physics-Dosimetry Support for the PSF Experiments", NUREG/CR-3318 Revision 5, USNRC, September (1984).
9. W. T. Urban et al., "Pool Critical Assembly Benchmark Solutions Using MCNP and THREEDANT", *The 8th ASTM-Euratom Symposium on Reactor Dosimetry*, Vail, Colorado, 29 Aug.-3 Sept., pp. 376-383 (1993).
10. J. P. Both et al., "A survey of TRIPOLI-4", *8th ICRS*, pp.373-377 (1994).
11. Y. K. Lee et al., "Validation of Monte Carlo Code TRIPOLI-4 with PWR Critical Lattices by Using JEF2.2 and ENDF/B-VI Evaluations", *M&C and SNA '97*, Saratoga, NY, 5-9 Oct., pp.253-262 (1997).
12. Y. K. Lee, "Evaluation of CRISTO-II Storage Arrays Benchmark with TRIPOLI-4.2 Criticality Calculations", *Advanced Monte Carlo on Radiation Physics, Particle Transport Simulation and Applications (MC 2000)*, Lisbon, Portugal, 23-26 Oct., pp. 809-814 (2000).
13. Y. K. Lee et al., "A Gamma Heating Calculation Methodology for Research Reactor Application", *5th Int. Topical Meeting on Research Reactor Fuel Management (RRFM 2001)*, Aachen, Germany, 1-3 Apr., pp. 147-151 (2001).
14. J. P. Both et al., "Automatic Importance Generation and Biasing Techniques in TRIPOLI-3", *Prog. In Nuclear Enegry*, **24**, pp. 273-281 (1990).
15. Y. Pénéliau and J. P. Both, "Parallelization of the Monte Carlo Code TRIPOLI-4", *M&C'99*, Madrid, Spain, 27-30 Sep., pp. 411-421 (1999).
16. E. M. Zsolnay and H. J. Nolthenius, "Analysis and Inter-comparison of the Cross Section and Related Uncertainty Data Present in the Reactor Dosimetry Libraries IRDF-90, JENDL/D-99 and RRDF-98", IAEA/INDC(NDS)-435, Vienna, Austria, 27-29 Aug., pp.31-37 (2002).
17. D. G. Madland, "The Los Alamos Model of Neutron Emission in Fission", *Heavy Ion Physics*, **10**, pp. 231-240, (1999).
18. D. Beretz et al., "French PWR Pressure Vessel Surveillance Program Dosimetry: Experience Feedback from More Than a Hundred Capsules", *10th ISRD*, pp.29-37 (1999).